

# INTEGRATED PHASE-INTERROGATION LN OPTICAL WAVEGUIDE SENSOR

Ruey-Ching Twu and Hong-Yao Hou

Department of Electro-Optical Engineering, Southern Taiwan University of Science and Technology, Tainan 710, Taiwan; Corresponding author: rctwu@mail.stust.edu.tw

Received 27 November 2012

**ABSTRACT:** We develop a phase interrogation optical waveguide sensor by integrating a phase modulator and a sensing transducer fabricated with the same Zn-indiffused lithium niobate substrate. The proposed sensing chip effectively reduces the footprint of the measurement setup and has the potential to provide a compact module for a portable metrology system. © 2013 Wiley Periodicals, Inc. *Microwave Opt Technol Lett* 55:1821–1823, 2013; View this article online at [wileyonlinelibrary.com](http://wileyonlinelibrary.com). DOI 10.1002/mop.27694

**Key words:** homodyne metrology; phase modulator; waveguide sensor

## 1. INTRODUCTION

Optical waveguide sensors based on evanescent field sensing schemes have been of great interest for applications in many areas, such as biosensing, temperature, and pressure sensors [1–4]. The three different techniques for measuring the optical signals when determining the sensing parameters are: optical intensity, phase, and spectra interrogations. In the intensity interrogation, the measurement setup is simple and the response time is fast; however, the resolution is limited by laser power variations and environmental noise. The spectra analysis, which requires an expensive broadband light source and a spectrometer, can provide a higher resolution but has a lower response time when compared with the intensity interrogation scheme. In comparison with the intensity and the spectra interrogations, the phase interrogation utilizing the homodyne or heterodyne methods can obtain precise resolutions and acceptable measurement speeds.

In the past decade, waveguide sensing transducers for optical sensing have been fabricated using various substrate materials, including: glass [4], silicon [3], and lithium niobate (LN) [5]. Glass transducers are cheap and disposable; however, they are difficult to integrate into an optical phase modulator on the same chip for homodyne or heterodyne metrology. The silicon semiconductor substrate can modulate the refractive indices of the waveguide by changing the carrier concentrations based on a p-i-n diode structure [6]. While it is possible to combine it with a phase modulator and waveguide transducer on the same chip, the process integrations are complicated and the costs higher. The propagation loss of the silicon semiconductor substrate is high at visible wavelengths; thus, silicon sensing chips have been primarily used for the near-infrared wavelengths. The LN substrate can be used for tunable phase retarders due to its essential birefringence and great electro-optic effects; in addition, its unique properties fit those required for a waveguide sensor [5]. However, the pyroelectric (PE) and photorefractive (PR) properties of the LN substrate impact the phase stabilities of the propagating lights in the channel waveguides [7]. Moreover, the PE and PR effects are also dependent on the relationship between the lightwave propagation direction and the optic-axis of the LN substrate. An x-cut/z-propagating waveguide device has proven to have the best phase stabilities for the LN substrate [8]. Thermally Ti-indiffused LN (TILN) waveguide devices have numerous commercial applications in the field of fiber optical communications. However, because of the obvious

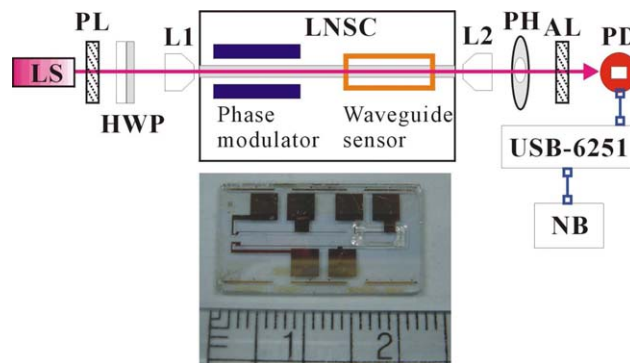


**Figure 1** Schematic diagram of the measurement setup. [Color figure can be viewed in the online issue, which is available at [wileyonlinelibrary.com](http://wileyonlinelibrary.com)]

PR effects, TILN waveguide phase modulators are unsuitable for optical metrology operating at visible wavelengths. Recently, various Zn-indiffused LN (ZILN) waveguide devices have been proposed for high-efficiency wavelength converters or stable mode converters at visible wavelengths [9,10]. Moreover, the stable ZILN phase modulators have been used for homodyne and heterodyne instruments [11,12].

This study, for the first time, successfully demonstrates a compact sensing chip in ZILN substrate. The repeatable measurements were achieved by putting the ethanol testing solutions onto the surface of the sensing transducers. Unlike the separated arrangement of the phase modulator and the sensing transducer, the proposed LN sensing chip (LNSC) easily integrated these two functional elements on the same chip. Moreover, the compact metrology module could be packaged with the photonic devices and signal processing chips on the same board for a portable instrument.

## 2. MEASUREMENT SETUP

Figure 1 depicts the schematic measurement setup. The inset is a photograph of the fabricated LNSC. An He–Ne laser (LS) at 632.8 nm was adopted for the optical sensing. Linearly polarized light, at 45° with respect to the horizontal axis of the laboratory coordinates, was obtained after having passed through a polarizer and a half-wave plate. The incident light was coupled into the LNSC through an objective lens (L1). The propagating light passed through, sequentially, an embedded phase modulator and a sensing transducer in the LNSC. The output light was collected using another lens (L2). A pinhole (PH) was used to block the scattering lights from the L2. The output light was received by a photodetector after an analyzer. The converted electrical signal was sent to a data acquisition box (USB-6251), which was connected to a notebook personal computer (NB). The signal process and measured phase variation were performed in a LabVIEW-based environment [11].

The proposed LNSC was fabricated using the thermally Zn-indiffused waveguide in the x-cut/z-propagating LN substrate. Details of the fabrication have been described in the reported paper [10]. The width and length of the fabricated channel waveguide were 4  $\mu\text{m}$  and 22 mm, respectively. After the waveguide fabrication, the phase modulation electrodes were deposited on the side of the channel waveguide. The length and gap of the parallel electrodes were 12 mm and 14  $\mu\text{m}$ , respectively. The electrodes were protected by a silicon dioxide ( $\text{SiO}_2$ ) cladding layer of 300 nm. The sensing area of the waveguide was not covered by the cladding layer. UV-curing glue, with a

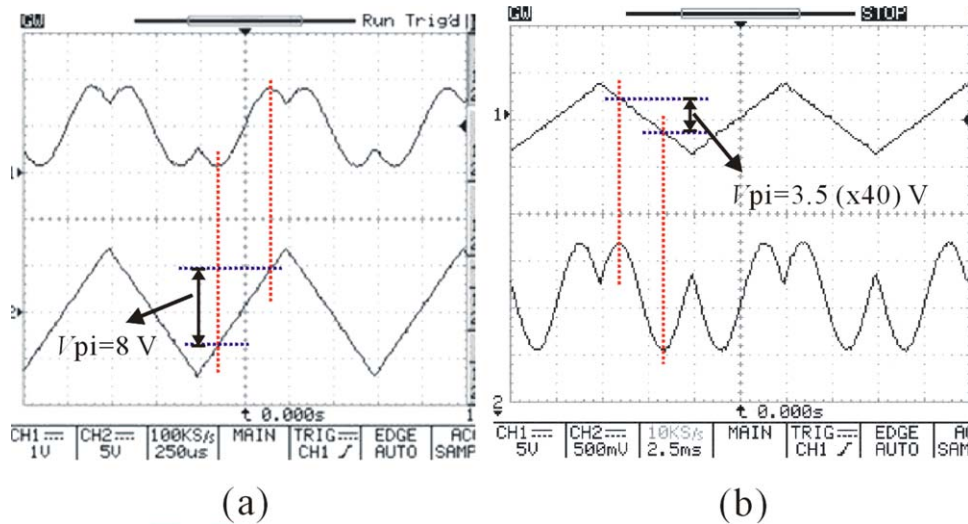


**Figure 2** Applied voltages and optical response curves for the phase modulator: (a) LNSC and (b) EOM. [Color figure can be viewed in the online issue, which is available at [wileyonlinelibrary.com](http://wileyonlinelibrary.com)]

rectangular dam of  $4 \times 8 \text{ mm}^2$  and a height of about 1 mm, was used to confine the test liquid, which was injected with a syringe onto the surface of the sensing area.

### 3. RESULTS AND DISCUSSIONS

The fabricated phase modulator in the LNSC was measured for a switching voltage,  $V_{\pi}$ , defined as an applied voltage to obtain a half-wave phase shift between two orthogonal polarizations. As shown in Figure 2(a), the measured  $V_{\pi}$  was 8 V, according to the relations between the applied voltage and the optical response curve. At the same input wavelength of 632.8 nm, the measured  $V_{\pi}$  of a commercial buck-type EOM (New Focus 4002) was 140 V, as shown in Figure 2(b). In comparison with the commercial EOM, the embedded phase modulator of the LNSC had a relatively lower voltage operation. In the homodyne technique, the applied modulation peak voltage was less than  $V_{\pi}$ . Therefore, the applied ac voltage was 5 V with a frequency of 100 Hz for the optical phase measurements in the proposed LNSC. This low applied voltage could be easily integrated onto low-power electronic chips.

By utilizing the proposed homodyne technique [11], the phase stabilities of the LNSC and EOM were evaluated under

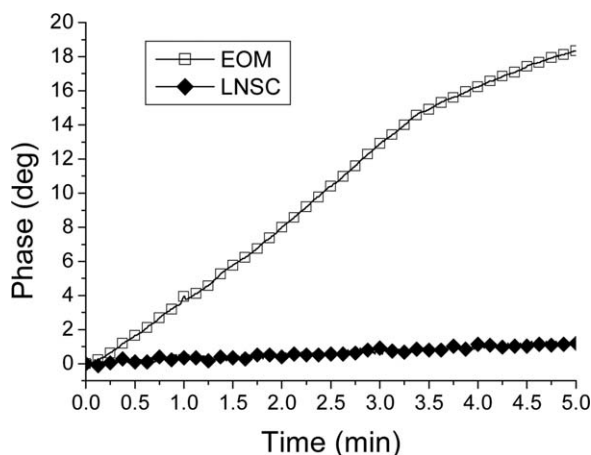


**Figure 3** Measurement results of the phase stability for the LNSC and EOM

the same throughput optical power of  $25 \mu\text{W}$  and a phase modulation depth of 1.96 for 5 min, as shown in Figure 3. The maximum phase changes were 18 and  $0.9^\circ$  for the EOM and the LNSC, respectively. The phase variation of the EOM was obvious as compared with that of the LNSC. Figure 4 presents the phase variations of the LNSC under the ambient temperature changes. The chip was placed onto a plate heater and the temperature change was monitored through a thermal probe. The phase change was around  $4.5^\circ$  for temperature variations ranging from 24.5 to  $29^\circ\text{C}$ . The thermally induced phase change rate of the LNSC was around  $1.5^\circ/\text{C}$ .

In the evanescent field sensing scheme, without the liquids on the waveguide surface, the tail of the evanescent field was near the air-LN boundary. The evanescent tail was enhanced in the covered region when the liquids were injected. Therefore, only the transverse-magnetic (TM)-polarized mode underwent increased propagation time and thus caused the increments of phase delay between the transverse-electric and the TM polarizations. Figure 5 shows the phase variations for the different injecting liquids. First, a droplet of deionized water was injected onto the sensing area at 60 sec, and the phase jump was around  $1.6^\circ$ , as shown in Figure 5(a). After the injection, only minor phase changes ( $<0.5^\circ$ ) were observed due to the very low

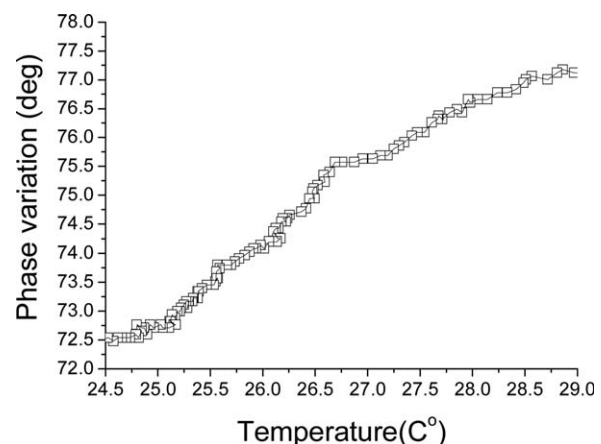


**Figure 4** Phase variation as a function of ambient temperature

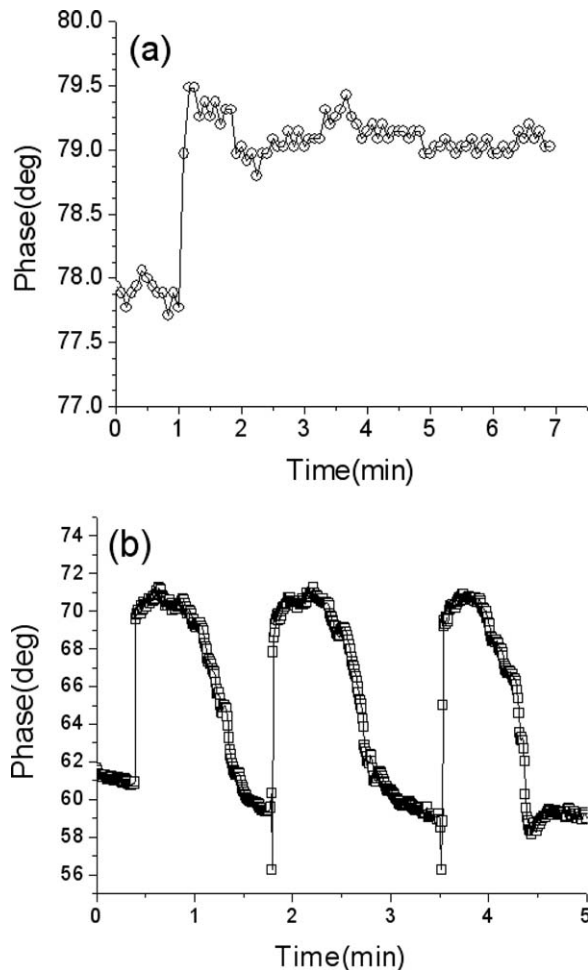


**Figure 5** Phase variations for different liquids: (a) deionized water and (b) ethanol

evaporation rate of the covered water. This also meant that the phase stabilities of the LNSC dropped below  $0.5^\circ$ . To ensure the repeatability of the measurements in a short period, we injected the ethanol liquid three times at 25, 110, and 210 sec, as shown in Figure 5(b). In the initial period after the ethanol injection, the average phase change for the three injections was about  $11^\circ$ . Then, the phase values returned to the original level due to the complete evaporation of the ethanol liquid. The results indicated that the phase measurements were repeatable and stable. The dynamic evaporation of the ethanol liquid was readily observed.

#### 4. CONCLUSION

We developed an optical phase tunable sensing chip by integrating a phase modulator and an evanescent waveguide transducer in the same LN substrate. The homodyne phase interrogation has been successfully demonstrated to measure repeatable phase variations during the evaporation of the ethanol solutions injected onto the waveguide transducer. Most notably, the properties of a low driving voltage and stable phase operation have underlined the merit of developing ZILN-based waveguide sensors for use in portable instruments.

#### ACKNOWLEDGMENT

This work was supported by the National Science Council, Taiwan (NSCT), under Grants NSC 99-2221-E-218-028 and NSC 100-2221-E-218-034-MY3.

#### REFERENCES

1. K. Schmitt, K. Oehse, G. Sulz, and C. Hoffmann, Evanescent field sensors based on tantalum pentoxide waveguides—A review, *Sensors* 8 (2008), 711–738.
2. B.J. Luff, J.S. Wilkinson, J. Piehler, U. Hollenbach, J. Ingenhoff, and N. Fabricius, Integrated optical Mach–Zehnder biosensor, *J Lightwave Technol* 16 (1998), 583–592.
3. A. Irace and G. Breglio, All-silicon optical temperature sensor based on Multi-Mode Interference, *Opt Express* 11 (2003), 2807–2812.
4. H. Nikkuni, Y. Watanabe, M. Ohkawa, and T. Sato, Sensitivity dependences on side length and aspect ratio of a diaphragm in a glass-based guided-wave optical pressure sensor, *Opt Express* 16 (2008), 15024–15032.
5. T.J. Wang and C.W. Hsieh, Surface plasmon resonance biosensor based on electro-optically modulated phase detection, *Opt Lett* 32 (2007), 2834–2836.
6. Q. Xu, S. Manipatruni, B. Schmidt, J. Shakya, and M. Lipson, 12.5 Gbit/s carrier-injection-based silicon micro-ring silicon modulators, *Opt Express* 15 (2007), 430–436.
7. M. Aillerie, M.D. Fontana, F. Abdi, C. Carabatos Nedelec, N. Theofanous, and G. Alexakis, Influence of the temperature-dependent spontaneous birefringence in the electrooptic measurements of LiNbO<sub>3</sub>, *J Appl Phys* 65 (1989), 2406–2408.
8. S. Thaniyavarn, Wavelength independent, optical damage immune z-propagation LiNbO<sub>3</sub> waveguide polarization converter, *Appl Phys Lett* 47 (1985), 674–677.
9. L. Ming, C.B.E. Gawith, K. Gallo, M.V. O'Connor, G.D. Emmerson, and P.G.R. Smith, High conversion efficiency single-pass second harmonic generation in a zinc-diffused periodically poled lithium niobate waveguide, *Opt Express* 13 (2005), 4862–4868.
10. R.C. Twu, H.H. Lee, H.Y. Hong, and C.Y. Yang, A novel Zn-indiffused mode converter in x-cut lithium niobate, *Opt Express* 15 (2007), 15576–15582.
11. R.C. Twu, H.H. Hong, and H.H. Lee, Dual-channel optical phase measurement system for improved precision, *Opt Lett* 33 (2008), 2530–2532.
12. R.C. Twu, Y.H. Lee, and H.Y. Hou, A comparison between two heterodyne light sources using different electro-optic modulators for optical temperature measurements at visible wavelengths, *Sensors* 10 (2010), 9609–9619.

© 2013 Wiley Periodicals, Inc.

## A DUAL-BAND BANDPASS FILTER USING CAPACITIVELY I/O COUPLING

Jahyeon Lee and Yeongseog Lim

Department of Electronics and Computer Engineering, Chonnam National University, Gwangju, South Korea; Corresponding author: spiritofpastmemory@gmail.com

Received 27 November 2012

**ABSTRACT:** A compact microstrip dual-band bandpass filter with good frequency selectivity was proposed. The proposed dual-band bandpass filter is configured with two dual-mode resonator and skew-symmetrically coupled capacitively input/output coupling. By using these input/output coupling structure, extra transmission zeros can be generated. The dual-band bandpass filter is designed for 2.4/5.2 GHz WLAN. Experimental measurements are also presented for the validation of the theory. © 2013 Wiley Periodicals, Inc. *Microwave Opt Technol Lett* 55:1823–1825, 2013; View this article online at wileyonlinelibrary.com. DOI 10.1002/mop.27693

**Key words:** filter; dual-band filter; capacitive coupling

#### 1. INTRODUCTION

The development of the modern communication systems requires microwave components to operate in either dual-band